Spontaneous Structural Transition in Phospholipid-Inspired Aromatic Phosphopeptide Nanostructures

Michal Pellach,[†] Yoav Atsmon-Raz,[‡,§] Eyal Simonovsky,[‡,§] Hugo Gottlieb,[⊥] Guy Jacoby,[∥] Roy Beck,[∥] Lihi Adler-Abramovich,[†] Yifat Miller,[*,‡,§] and Ehud Gazit[*,†,#]

[†]Department of Molecular Microbiology and Biotechnology, George S. Wise Faculty of Life Sciences, Tel Aviv University, Tel Aviv 69978, Israel, [‡]Department of Chemistry, Ben-Gurion University of the Negev, Be'er Sheva 84105, Israel, [§]Ilse Katz Institute for Nanoscale Science and Technology, Ben-Gurion University of the Negev, Be'er Sheva 84105, Israel, [⊥]Department of Chemistry, Bar-Ilan University, Ramat Gan 52900, Israel, [∥]The Raymond and Beverly Sackler School of Physics and Astronomy, Tel-Aviv University, Tel-Aviv 69978, Israel, and [#]Department of Materials Science and Engineering Iby and Aladar Fleischman Faculty of Engineering, Tel Aviv University, Tel Aviv 69978, Israel

ABSTRACT Phospholipid membranes could be considered a prime example of the ability of nature to produce complex yet ordered structures, by spontaneous and efficient self-assembly. Inspired by the unique properties and architecture of phospholipids, we designed simple amphiphilic decapeptides, intended to fold in the center of the peptide sequence, with a phosphorylated serine "head" located within a central turn segment, and two hydrophobic "tails". The molecular design also included the integration of the diphenylalanine motif, previously shown to facilitate self-assembly and increase nanostructure stability. Secondary structure analysis of the peptides indeed indicated the presence of stabilized conformations in solution, with a central turn connecting two hydrophobic "tails", and interactions between the hydrophobic strands. The mechanisms of assembly into supramolecular structures involved structural transitions between different morphologies, which occurred over several hours, leading to the formation of distinctive nanostructures, including half-elliptical nanosheets and curved tapes. The phosphopeptide building blocks appear to self-assemble *via* a particular combination of aromatic, hydrophobic and ionic interactions, as well as hydrogen bonding, as demonstrated by proposed constructed simulated models of the peptides and self-assembled nanostructures. Molecular dynamics simulations also gave insight into mechanisms of structural transitions of the nanostructures at a molecular level. Because of the biocompatibility of peptides, the phosphopeptide assemblies allow for expansion of the library of biomolecular nanostructures available for future design and application of biomedical devices.

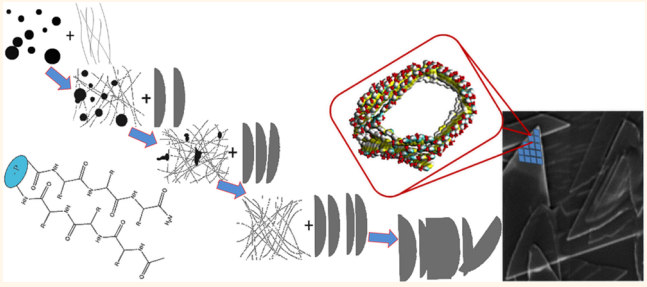

KEYWORDS: bioinspired design · peptides · self-assembly · phosphorylation · nanostructures · molecular dynamics simulation

Phospholipids are most recognized for their importance in the self-assembly of biological membranes *via* the hydrophobic effect. These membranes allow for cellular formation and function as well as compartmentalization of organelles.[1] Phospholipids may also be arranged into various micro- and nanostructures, and besides liposomes (unilamellar vesicles) that mimic the eukaryotic cell membrane and the phospholipid bilayer, lipid assemblies also include micelles, multilamellar vesicles, thin bilayer films and tubular structures.[2,3] Phospholipids have thus been the inspiration for numerous self-assembling amphiphilic building blocks. Another nature-inspired growing field is the self-assembly of peptides. While the predominant force that leads to lipid self-assembly is the hydrophobic effect, peptides interact *via* hydrophobic interactions as well as hydrogen bonding, aromatic interactions, ionic interactions and van der Waals forces, and depend on both the primary amino acid sequence as well as secondary structure. Examples of self-assembled peptide morphologies include β-sheet fibers, ribbons, nanospheres and nanotubes.[4−6]

Naturally, lipids organize into different molecular arrangements such as micellar, lamellar, hexagonal or isotropic molecular organization, and undergo transitions

* Address correspondence to ymiller@bgu.ac.il, ehudg@post.tau.ac.il.

Received for review January 8, 2015 and accepted March 24, 2015.

Published online March 24, 2015
10.1021/acsnano.5b00133

between different phases. Hexagonal (H) phases consist of lipid cylinders (H_I with a hydrophobic core and H_{II} with a hydrophilic core), and cubic phases are quasi-crystalline, three-dimensional, optically isotropic arrangements. The preferred lipidic arrangement is influenced by a variety of factors such as temperature, pH and ionic strength.[7] Lipid polymorphism and self-assembly has been explored in nanomedicine for drug delivery applications.[8−10] In addition, synthetic lipid nanotubes are usually formed from helically wrapped lipid bilayers. Nanotube formation from amphiphilic molecules generally requires highly ordered molecular packing as well as anisotropic molecular interactions.[2,11] Theoretically, the chirality of the molecule results in an energetically favored orientation and packing at a nonzero angle relative to its neighbor. This then results in the twisting of a bilayer and may result in the formation of a hollow tube. Lipid nanotubes have been produced by self-assembly of both natural and synthetic lipids with phosphocholine, sugar, peptide or nucleic acid headgroups.[12]

Several examples of lipid-mimicking peptides have been described to autonomously form nano- and microstructures, and fall under a general category of amphiphilic or "lipid-like" peptides.[13−15] These may be composed solely of amino acids with hydrophilic sidechains forming the hydrophilic head and hydrophobic residues forming the tail, such as those developed by the Zhang research group.[13] Some expansion of this work has demonstrated that variation of the number or type of residues that form the hydrophobic tail or hydrophilic head can be used to control the architecture of the assemblies.[16,17] In addition, a vast collection of "peptide amphiphiles" has been developed by Stupp and co-workers, in which an alkyl chain is appended to a generally hydrophilic peptide sequence. Their alkyl tails self-associate resulting in the formation of peptidic fibers with a core comprised of alkyl chains, a peptide β-sheet-forming segment, and a surface that displays a biologically active epitope.[18] The research group of Schneider has developed an additional class of amphiphilic peptides with β-hairpin secondary structure, and alternating between hydrophilic and hydrophobic residues creates a hydrophilic face and a hydrophobic face. The hydrophobic faces associate to form bilayers, which self-assemble into β-sheet fibrils that then form hydrogels.[19,20]

Aromatic moieties have substantial influence on the self-assembly of peptides and lipidic molecules. Specifically, since reports of self-assembly of the dipeptide diphenylalanine into nanostructures,[21] a vast number of diphenylalanine analogues have been synthesized to form a variety of self-assembling nanostructures.[4,22] The formation of supramolecular aggregates from fatty acids or phospholipids with aromatic chromophores incorporated into the sidechains have been studied, and it has been shown that supramolecular assembly formation is accompanied by formation of aggregates of the aromatic group. Studies have indicated a close energetic balance between face−face and (perhaps favorable) edge−face aromatic interactions, and that these aromatic interactions could be used for the control of various molecular assemblies.[23,24]

While zwitterionic amphiphilic lipids constitute the main building blocks for biological membranes, and are sufficient for membrane stabilization, biomembranes are also known to contain a significant proportion of negatively charged phospholipids. The negative charge has a destabilizing effect, and their critical micelle concentration is greatly increased relative to zwitterionic phosphatidylcholine or to high-ionic-strength conditions.[25] Besides affecting the self-assembly of lipids, phosphate functionality is significant in peptides and proteins. It has exhibited capability of inducing changes in self-assembly behavior of proteins such as tau protein, and tau-related amyloid fibrils.[26−28] Phosphorylation or dephosphorylation can be enzymatically controlled, and kinases and/or phosphatases have been utilized for triggering the formation and/or deformation of coiled coil peptides,[29,30] peptide nanotubes,[31] peptide amphiphile fibers,[32] and fibrils from polymer−peptide conjugates.[33]

In the current work we aimed to mimic phospholipid architecture with an oligopeptide possessing a hydrophilic "head" and two hydrophobic "tails". Previously designed amphiphilic or lipid-like peptides generally rely on hydrophobicity and hydrophilicity of the amino acids, and the hydrophobic effect. Here, for the first time, the diphenylalanine moiety was incorporated into two hydrophobic tails of an amphiphilic peptide, allowing intra- and intermolecular aromatic interactions into the self-assembly process. In addition, a phosphate group was integrated for resembling the phospholipid headgroup. Phosphorylation of the peptide was expected and demonstrated to significantly affect peptide self-assembly. These phosphopeptide building blocks were discovered to undergo structural transition from spheres to fibrils and then to two different novel structural morphologies: curved nanotapes and half-elliptical nanosheets.

RESULTS AND DISCUSSION

Peptide Design. Our peptide design involved the usage of natural amino acids to form a phospholipid-inspired two-tailed amphiphile, with a phosphorylated serine as the polar "head" (Figure 1). We used a 10-amino acid peptide chain, with a Pro-Ser β-turn. On either side of the turn, oppositely charged Lys and Glu were included for drawing together the hydrophobic tails, each consisting of Val, which has high propensity for β-sheet formation, and Phe-Phe. Adjacent to the β-turn were therefore chains of increasing hydrophobicity. Diphenylalanine has been well-studied and found to form particularly strong intermolecular

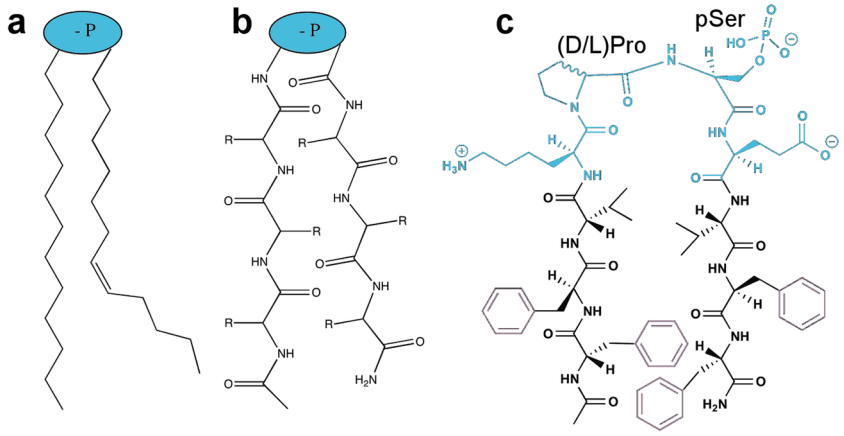

Figure 1. Design of phospholipid-inspired phosphopeptides. (a) Representation of a phospholipid, consisting of a polar phosphorylated head and two aliphatic tails. (b) Replacement of aliphatic chains with peptidic chains, potentially substituting a self-assembling phospholipid with a self-assembling peptide. (c) Designed peptide sequence. The hydrophilic region of the designed peptide is composed of four residues: lysine, proline (D or L), phosphoserine and glutamic acid. A phosphorylated hydrophilic "head" is thus created, to give resemblance of the "head" of a phospholipid. The well-studied diphenylalanine motif is incorporated into each of the hydrophobic tails. Diphenylalanine possesses high propensity for self-assembly, previously demonstrated to form intermolecular aromatic interactions. Besides intermolecular interactions, when placed at each end, the aromatic moieties would also allow for intramolecular aromatic interactions, thus increasing the likelihood of interactions between the two hydrophobic "tails", and folding of the peptide at the hydrophilic head.

interactions involving the aromatic moieties. In the phosphopeptides studied in this work, the aromatic interactions could potentially occur both intramolecularly, increasing interaction between hydrophobic "tails" and intermolecularly, strengthening possible self-assembled structures.

While the usage of all-L-amino acids could be considered somewhat more resemblant of the phospholipids found in biomembranes, in that the two phospholipid alkyl chains are not directly aligned with one another, usage of (D)Pro in the turn at the phosphopeptide head could fulfill stereochemical requirements for alignment of each of the "tails", allowing intramolecular hydrogen bonding and β-sheet formation, and therefore yielding a β-hairpin structure. Two peptides, one with (D)Pro and the other with (L)Pro were explored, the resulting sequences of which were Ac-Phe-Phe-Val-Lys-(D)Pro-pSer-Glu-Val-Phe-Phe-NH_2 (D-phosphopeptide) and Ac-Phe-Phe-Val-Lys-(L)Pro-pSer-Glu-Val-Phe-Phe-NH_2 (L-phosphopeptide), where pSer is phosphoserine.

With the use of (D)Pro in the peptide sequence, allowing for fulfillment of sterochemical requirements for β-hairpin formation, this could also allow for aromatic interactions between the two sides of the molecule. Aromatic interactions between β-sheet strands of β-hairpins have been previously studied,[34−38] and are generally accepted to be stabilizing of β-hairpin structures.[37,39] It has been observed that the aromatic rings are in close proximity (roughly 4.8−5.5 Å) when the Phe residue is placed either at corresponding hydrogen bonded position (between two intramolecular hydrogen bonds) or non-hydrogen-bonded positions, which are favored.[35,36] In the D-phosphopeptide, (with the D-Proline allowing for interstrand hydrogen bonding), The Phe-2 and Phe-9 residues are in hydrogen bonding positions, whereas Phe-1 and Phe-10 are in non-hydrogen-bonding positions.

Peptide Secondary Structure Analysis. NMR studies were performed in solution for determining whether the phosphopeptides adopt conformations that may resemble or mimic the phospholipid "head" and "tails" as a result of intramolecular interactions. (NMR assignments are available in Tables S1−S5, Supporting Information.) Two solvents were used for the study: trifluoroethanol (TFE), a stabilizer of secondary structure,[40,41] and DMSO for comparison. In TFE, for both peptides, there is indeed indication of a stabilized conformation for each peptide, characterized by interresidue nuclear Overhauser effects (NOEs). Presence of the clearly visible interresidue NOEs indicate that the "folded" conformation is the dominant conformation in solution. There is also evidence that for both isomers there are interactions between the two sides of the molecule (*i.e.*, amino acids 1−4 with 6−10).

Despite their almost identical amino-acid sequence, (differing only in the stereochemistry of the prolines,) in their stabilized conformations in TFE, amide protons belonging to the peptide backbone of the D-phosphopeptide fall at significantly higher chemical shifts compared to those of the L-phosphopeptide. This could be a result of the intramolecular hydrogen bonding expected for the D-phosphopeptide, between β strands of a β-hairpin. Additional evidence supporting β-hairpin formation is the prominent NOE observed from interaction between the amide proton of Lys-4 (8.60 ppm) and a β proton of Glu-7 (2.32 ppm), indicating that (D)Pro-5 and pSer-6 form the β turn. The L-phosphopeptide does not possess stereochemistry that allows for β-hairpin conformation; however, in

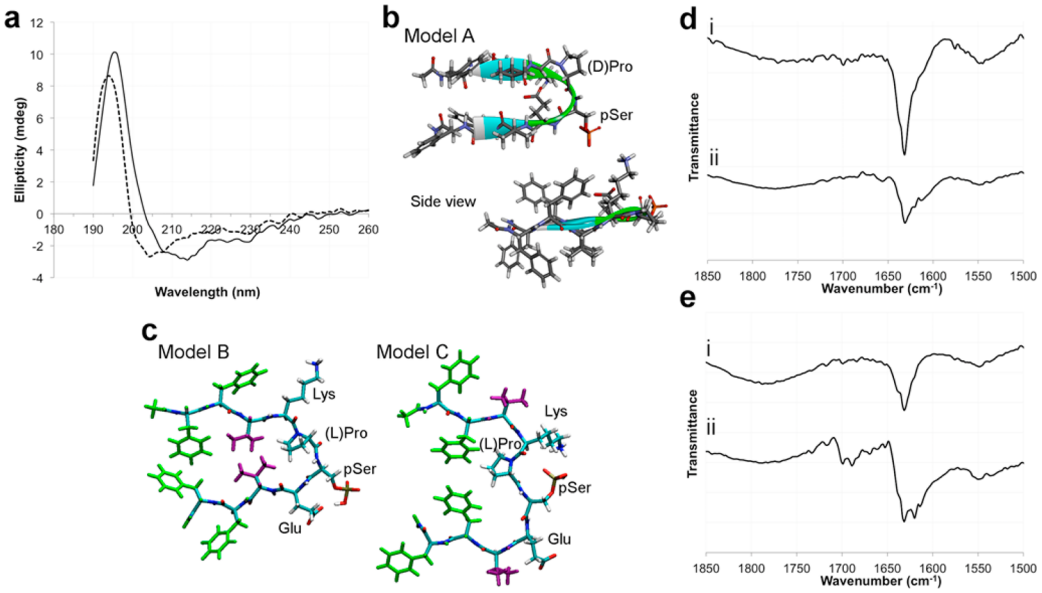

Figure 2. Characterization of phosphopeptide secondary structure. (a) CD spectra in TFE. Solid line: D-phosphopeptide, dashed line: L-phosphopeptide. Both peptides in solution give a general curve indicating β-sheet structure. The CD spectrum of the D-phosphopeptide gives a maximum and minimum of 195 and 213 nm, respectively, typical of β-sheet structure. The L-phosphopeptide has a shifted spectrum, with a maximum at 194 nm and a minimum at 205 nm. Despite lack of intramolecular hydrogen bonding, the spectrum shape may be the result of two β-strands brought together by hydrophobic and/or aromatic sidechain interactions. (b) Top and side view of the constructed model of the D-phosphopeptide (Model A, Supporting Information). The peptide adopts a β-hairpin conformation with intramolecular hydrogen bonding, forming a β-sheet. (c) Constructed models of the L-phosphopeptide adopting β-arch Model B (left) and β-arch Model C (right) (details in Supporting Information). Noteworthy are the possible aromatic interactions between Phe-1-Phe-10 in Model B and Phe-2-Phe-9 in Model C. (d) FTIR Spectra of the D-phosphopeptide from a dried TFE solution (i), and after HFIP/Water solvent exchange and self-assembly into half-elliptical nanosheets (ii). The peak at 1631 cm^{-1} is indicative of β-sheet structure, and no significant differences are observed between the spectra. (e) FTIR Spectra of the L-phosphopeptide from a dried TFE solution (i), and after HFIP/Water solvent exchange and self-assembly into curved nanotapes (ii). According to the FTIR spectrum, β-sheet structure is retained after self-assembly, with additional peaks appearing for the L-phosphopeptide at 1620, 1689 and 1699 cm^{-1}, possibly indicating a change in character of the β-sheet structure.

TFE, a specific conformation is observed, indicative of a turn in the hydrophilic region of the peptide. The most notable NOE observed supporting this theory is that which shows close proximity between the α proton of (L)Pro-5 (4.26 ppm) and the sidechain CH_3 protons of Val-8 (0.86 ppm).

In DMSO the phosphopeptides had completely different behavior compared to that in TFE. While for the NMR spectra in TFE almost complete proton allocation could be achieved, in DMSO the interpretation of the NMR spectra was much more difficult. The two reasons for the difficulties were, first, the broadening of peaks, indicating two or more conformations in medium-rate equilibrium (barrier *ca.* 13−14 kcal/mol), and second, for the D-phosphopeptide, two sets of peaks were observed indicating coexistence of two sets of conformations (*ca.* 80:20) in solution (barrier 15 kcal/mol or more). However, the existence of relatively stable conformers indicates some degree of interresidue stabilization. While at certain conformations NOEs would exist, their signal is significantly weakened with the presence of several conformations.

Prior to placement in self-assembling conditions, circular dichroism (CD) was performed in TFE, in order to obtain further information regarding the peptide secondary structure (Figure 2a). For the D-phosphopeptide, the stereochemistry would allow for intramolecular β-sheet formation. As expected, the positive peak at 195 nm together with the negative minimum at approximately 213 nm indicate β-sheet structure. In addition, both phosphopeptides presented a shoulder of the negative band, at 220−235 nm, which is similar to a spectrum previously described of peptides possessing a combination of a type II′ β-turn and β-sheet structure.[42] This further supports our suggestion that the D-phosphopeptide adopts a β-hairpin conformation with a type II′ β-turn, forming intramolecular hydrogen bonds between antiparallel strands belonging to the peptide backbone. Applying molecular modeling tools, the D-phosphopeptide was constructed with the folding of β-hairpin conformation as a "building block" (see Figure 2b and Supporting Information). Besides intramolecular hydrogen bonding, this β-hairpin model also allows for aromatic interactions between Phe-1 and Phe-10 as well as between Phe-2 and Phe-9.

For the L-phosphopeptide, the CD spectrum presented a slight blue-shift of the positive peak to 194 nm. Additionally, a negative minimum was

observed at approximately 205 nm, a lower wavelength than usually observed for typical β-sheet structure. A similar negative band, however, has been previously obtained for certain cyclic peptides possessing intramolecular β-sheets.[43] Unlike the cyclic peptides, in which β-hairpin turns were forced into the structure, it has been previously demonstrated that the β-hairpin structure (in noncyclic peptides) cannot be obtained from a turn that comprises (L)Pro-Xxx.[38] While the hydrophobic "tails" of the L-phosphopeptide cannot be present in sufficient proximity to allow for intramolecular H-bonding, the shape of the CD curve that resembles β-sheet structure might occur from hydrophobic and aromatic interactions between two β strands, which draw the strands in close proximity to each other. In order to exemplify the folding of the L-phosphopeptide into a stable conformation, we proposed that the folded L-phosphopeptide has a β-arch structure through which two β-strands are connected by a U-turn. The β-arch differs from the β-hairpin in that the two strands on either side of the turn are rotated so that they interact *via* their sidechains rather than *via* the peptide backbone.[44] Applying molecular modeling techniques, we constructed two different types of β-arch peptides as "building blocks" that differ in the shape of the turn. While in the β-hairpin D-phosphopeptide the intramolecular hydrogen bonds stabilize the peptide monomer, according to our model, in the L-phosphopeptide the intramolecular interactions that strongly contribute to the stability of the peptide monomer include hydrophobic interactions of Val-3-Val-8, aromatic interactions between Phe-1-Phe-10 and Phe-2-Phe-9, as well as salt-bridge interactions of Lys-4-Glu-7 (see Figure 2c and Supporting Information).

Furthermore, the phosphopeptides were characterized by FTIR to compare structural motifs for nonassembled phosphopeptide monomers as well as for the superstructures after the self-assembly process (Figure 2d). The D-phosphopeptide presented similar FTIR spectra from a dried TFE solution (in which the self-assembly process does not occur, but may allow for oligomerization during the drying process) and for the self-assembled nanosheets. Interestingly, for both the peptide "monomer" and superstructures a single peak is observed at 1631 cm^{-1} emphasizing distinct β-sheet structure, without significant change in character before and after the process of self-assembly into nanostructures.

The L-phosphopeptide (possibly oligomerized during the drying process) displayed peaks in both FTIR spectra that indicated presence of β-sheet structure, with peaks at 1631 cm^{-1}. Interestingly, in the 5% HFIP/Water conditions, following self-assembly (into nanotapes) there was appearance of additional peaks at 1620 cm^{-1} as well as at 1689 and 1699 cm^{-1}. These additional peaks suggest additional structural characteristics that appear as result of intermolecular interactions involved in the self-assembly process. Molecular Dynamics (MD) simulations (described in the following section) suggest the presence of β-sheet structure along the axis of the fibrils formed, and a twisting-like process that occurs during the structural transition between intermediate nanostructures.

Self-Assembly and Structural Transition. Self-assembly was performed for each of the peptides by solvent exchange from HFIP, in which the peptides are completely soluble, to water. In most cases, on addition of water there was immediate precipitation of spherical particles, presumingly due to the hydrophobic effect, as in phospholipid assembly, allowing hydrophobic moieties to face away from the water. This was followed by gradual formation of supramolecular structures, reaching their steady state structure over several hours. The D-phosphopeptide began as rounded structures, then formed fine fibers, which was followed by flat half-elliptal nanosheets. The L-phosphopeptide gradually formed nanotapes with a longitudinal curve (Figure 3).

The transition process of the D-phosphopeptide into fine fibers with a diameter of ~13−16 nm, followed by thin nanosheets occurred over 5−6 h. While the size of the nanosheets was not uniform, interestingly, the half-elliptical shape was quite uniform. This consisted of a straight, smooth edge, ranging from approximately 2 μm to over 40 μm, and a rough-edged curvature (Figure 3a). SEM and AFM showed that the structures are highly flexible, adopting the shape of structures beneath (such as fibers or additional nanosheets), with a thickness of around 10 $\pm$ 2 nm (Figure S1).

To provide an insight into the self-assembled fibrillar structures at the atomic resolution, we constructed two fibril-like tubular structural models with a diameter of ~15 nm (similar to the estimated diameter obtained from the TEM) of the self-assembled D-phosphopeptide adopting a β-hairpin conformation. In both fibril-like structures the (D)Pro and the pSer are located in the type II′ β-turn of the β-hairpin. In the one constructed fibril-like structure the pSer is outward facing, and in the second, facing inward. Details of the two constructed models are given in the Supporting Information. Interestingly, following MD simulations, in the simulated structure in which the pSer faced outward, all the self-assembled β-hairpin peptides remained intact *via* intermolecular hydrogen bonds and the diameter of the fibril-like structure was ~13−14 nm, similar to the estimated values from the TEM. In the simulated structure with the pSer facing inward, several intermolecular hydrogen bonds were broken. We therefore propose that the β-hairpin peptides are self-assembled with the β-turn oriented in the outer domain of the fibril-like structure (Figure 4a).

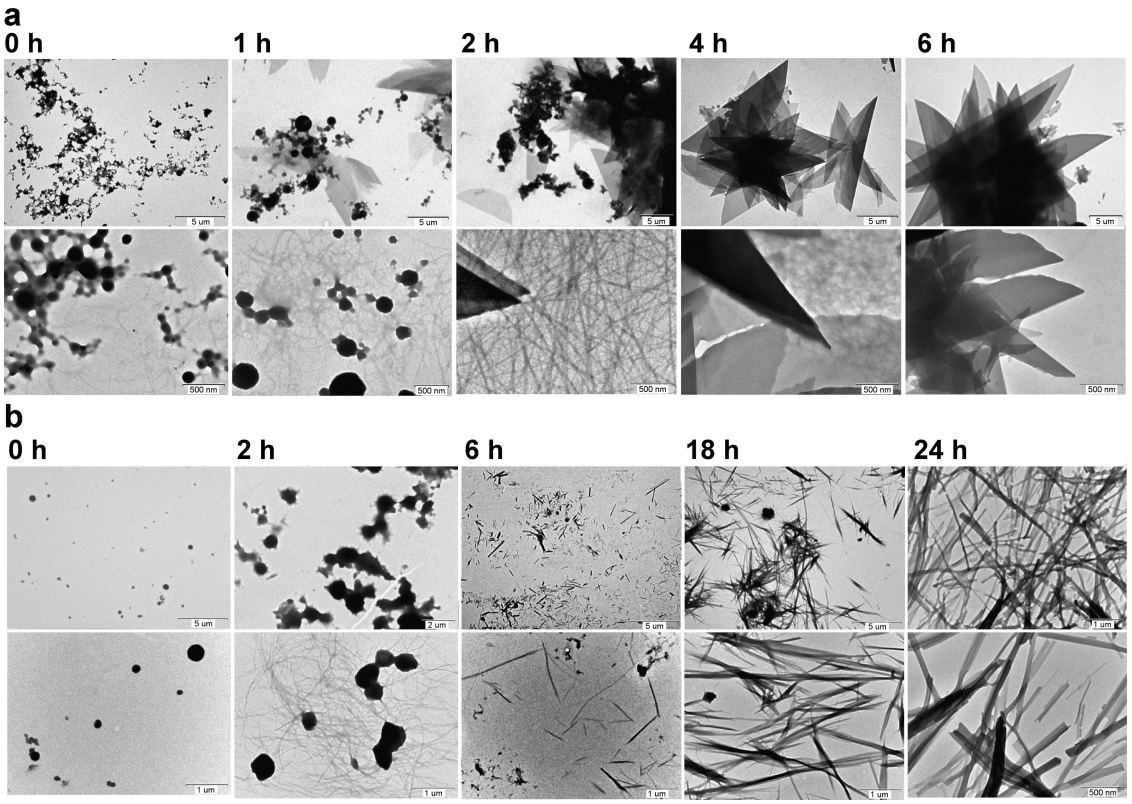

Figure 3. TEM images of structural transitions observed in the self-assembly process of the D-phosphopeptide (a) and the L-phosphopeptide (b). The self-assembly process is initiated by solvent switch from HFIP to water. The hydrophobicity of the peptides results in immediate precipitation and formation of spherical structures, and structural transition into fibers of approximately 13−17 nm in diameter, begins almost immediately. The diameters of the fibers were the starting point for the molecular dynamics (MD) simulations, which indicate reshaping of the fibers to form geometric shapes, giving a possible explanation for formation of half-elliptical nanosheets. While there was some variation in the dynamics of completion of the assembly process, the process involved transitions from spheres to fibers to half-elliptical nanosheets. For the L-phosphopeptide, the shortening and relengthening of nanostructures observed between the 6 and 18 h time points could be partially explained by MD simulations, which suggest several possible options for molecular rearrangement, involving weakening of intermolecular interactions, partial or complete opening of the fibrils, and formation of new intermolecular interactions. The final structures eventually formed, after approximately 24 h, resemble cinnamon sticks in shape.

Both simulated fibril-like structures revealed similar secondary structures as constructed in the initial structural models: two β-strands connected by a type II′ β-turn. The forces that stabilize this fibril-like structure along the cross-section of the fibril include intra- and intermolecular hydrogen bonding, aromatic interaction between the Phe groups and salt-bridge interactions between the Glu and Lys residues. The forces that stabilize the fibril-like structure along the fibril axis include aromatic interactions between the Phe groups and salt-bridge interactions between Glu and Lys residues (Figure S2). Following MD simulation, the fibril-like structure revealed two notable structural features. First, no twisting of the self-assembled β-hairpin peptides was observed, as commonly seen in amyloid peptides. The β-hairpins are organized as plated peptides that are connected *via* intermolecular hydrogen bonds. We propose that the organization of these peptides may explain the nanosheets observed by microscopy. Second, the simulated fibril-like structure demonstrated a polygonal structure (and not a circular tubule structure, as the initial fibril-structure had been constructed) with sharp angles. From the results of these MD simulations, we were able to propose a "stacked-tube" model, combining several polygons to form a semielliptical shape, which is a suggestion of the way the initial fibrils observed could eventually possess structural features observed in the final semielliptical nanosheets (Figure 4).

X-ray scattering was performed for concentrated D-phosphopeptide nanosheets in excess water. Prominent scattering peaks ($q_i = 2\pi/d_i$) that were observed indicated that the structures possess crystallinity, with repeating distances (d_i) of 4, 1.1, 0.96, and 0.46 nm (Figure 4c). The peak corresponding to 4 nm could correspond to a tail-to-tail bilayer. This value could also correspond to the height of a polygon-like structure with dimensions in the same order of magnitude as presented in the MD simulations. Another prominent peak corresponded to a 1.1 nm repeating distance. This could correspond to the distance between stacked β-hairpins (as depicted in Figure S2a, left-hand side), indicative of their face-to-face stacking. A peak corresponding to 0.96 nm may also be a "stacking" peak, for

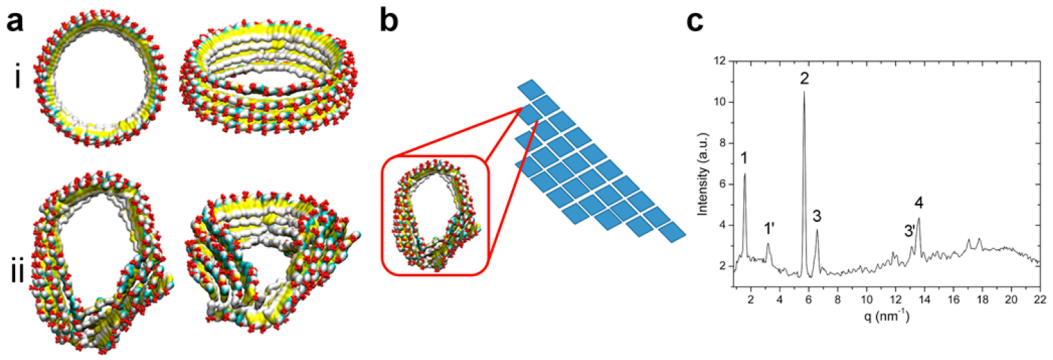

Figure 4. D-Phosphopeptide initial and final simulated tubular fibril-like structures and X-ray scattering spectrum. (a) Top-view (left) and side-view (right) constructed D-phosphopeptide early stage tubular fibril-like structures before (i) and after (ii) MD simulations. The tubular fibril-like structures are constructed with the pSer (in red) facing outward and the hydrophobic "tails" facing inward. Following MD simulations the tubular fibril-like structures are reshaped into polygonal structures. (b) Proposed schematic diagram illustrating a combination of polygonal structures to form a semielliptical shape. The early stage fibrillar structures thus present structural features observed in the flattened final-stage nanosheets. (c) X-ray scattering spectrum of D-phosphopeptide nanosheets, with peaks corresponding to repeating distances of 4, 1.1, 0.96, and 0.46 nm, denoted 1, 2, 3 and 4, respectively. The peaks corresponding to the second harmonic of 4 nm and of 1.1 nm are denoted 1′ and 3′, respectively.

perhaps slightly shifted or out-of-register stacking. Alternatively, this could be the repeating distance for a side-to-side arrangement (as depicted in Figure S2a top right) observed for the sides of the polygon in the proposed models. In addition, the momentum transfer vector, q = 13.6 nm^{-1} corresponds to d = 0.46 nm which is similar to the intra- and intermolecular distances between parallel β-stands of β-hairpins. Nevertheless, a first harmonic for such arrangement, should appear at q = 6.8 nm^{-1}, which we did not observe, so we have yet to resolve the 0.46 nm repeating distance. The X-ray scattering spectrum provided information regarding the molecular packing within the nanoplates, however, did not explain the semielliptical shape of the plates observed by TEM. The MD simulations were used to further explain the organization of the self-assembled peptides *via* an understanding of the fibrillar states. The MD simulations of the proposed fibrillar structures may provide an insight into the molecular organization to form the supramolecular structures.

There are few previous reports of self-assembled peptide plates or sheets. One example is the self-assembly of a homodipeptide formed from the non-natural amino acid, 4-phenyl-Phe. Di-4-phenyl-Phe assembled into square nanoplates, and their analysis by FTIR indicated both α-helical structure and turns or β-sheets.[45] Sheet-like structures have been formed at the air−water interface by peptides containing combinations of α and β amino acids,[46] as well as by amphiphilic β-hairpins.[47] Peptide nanosheets have also been previously described by Hamley *et al.*, in which the surfactant-like heptapeptide Ala_6-Arg formed nanosheets of 3 nm thickness, without evidence of intramolecular β-sheets.[48] In comparison, by microscopy, the current D-phosphopeptide nanosheets appear to be much larger, and unique in shape. The vibrational spectroscopy data, although indicative of β-sheet secondary structure, showed no additional peaks for the supramolecular structures, so additional intermolecular β-sheet interactions alone are not necessarily the forces that result in the nanosheet formation. While formation of a bilayer and intermolecular β-sheets between adjacent peptides would fit the flatness of the structures (interactions previously described for amphiphilic β-hairpins[47]), a bilayer does not fit the dimensions of the fibrillar structures at early stages of self-assembly nor the thickness (approximately 8−12 nm) of the nanosheets.

The L-phosphopeptide also appeared to transition from spheres into fibers (similar in diameter to those of the D-phosphopeptide, ∼13−17 nm); however, *via* what appeared as protrusions from the spherical structures. This then was followed by gradual formation of tape-like structures, with a longitudinal curvature. The final steady state was reached after approximately 24 h (Figure 3b). Similarly shaped partially formed tubes have been previously observed for lipid-like peptides; however, they were described to be nanotubes in the process of formation.[13] An assembly process showing the closure of open tubes has been suggested, and shown to be dependent on assembly conditions.[49,50]

To understand the self-assembly of the L-phosphopeptide at the atomic resolution, we constructed four fibril-like tubular structural models consisting of a β-arch peptide (comprised of two β-strands connected by U-turn/loop domain). We considered two types of β-arch peptide structures that differ in the shape of the U-turn (see Supporting Information and Figure 2c). The U-turn domains in each of the two types of the β-arch consist of (L)Pro and pSer. Applying each type of the two β-arch peptides, we proposed a total of four different fibril-like structures with diameters of ∼13 nm

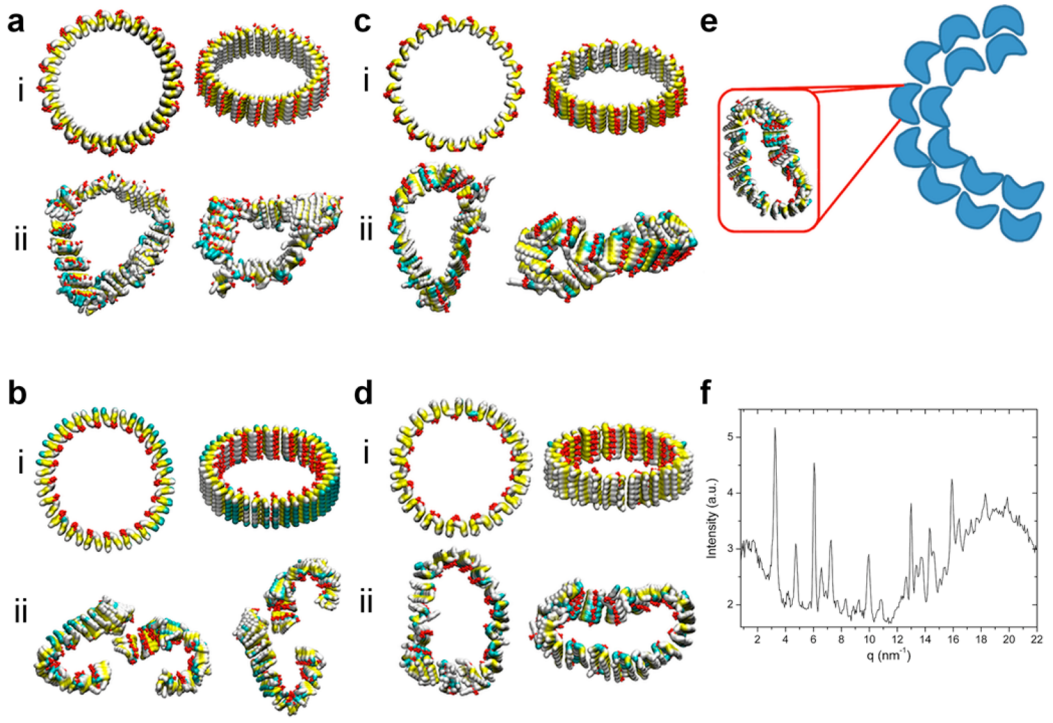

Figure 5. L-Phosphopeptide initial and final simulated tubular fibril-like structures and X-ray scattering spectrum. Top-view (left) and side-view (right) of four (a–d) constructed L-phosphopeptide structural models before (i) and after (ii) MD simulations. (a) Model B with pSer (in red) facing outward, (b) Model B with pSer facing inward, (c) Model C with pSer facing outward, and (d) Model C with pSer facing inward. β-sheet structure is retained along the fibril axis for all four simulations. The MD simulations portray a twisting-like process whereby intermolecular interactions are weakened at some point along the axis, leading to opening or partial opening of the structures, which would allow for formation of new intermolecular interactions between intermediate nanostructures. (e) Proposed schematic diagram of the formation of curved tapes from interactions between several "twisted" or "opened" fibrillar structures. (f) X-ray scattering spectrum of L-phosphopeptide nanotapes, displaying multiple scattering peaks including those corresponding to momentum transfer vectors (repeating distance) of 3.24 (1.94), 4.74 (1.32), 6.05 (1.04), 6.57 (0.96), 7.23 (0.87), 9.94 (0.63), 12.99 (0.48), 15.92 nm^{-1} (0.39 nm). These may belong to more than one ordered molecular arrangement.

(similar to the estimated values obtained from the TEM): two fibril-like structures in which the pSer is orientated facing outward, and two fibril-like structures in which the pSer is inward facing (Figure 5a–d). Details of the four constructed fibril-like structural models are given in the Supporting Information. Of the four constructed fibril-like structural models, following MD simulation, three models could retain their tubular structures, whereas the fourth (Figure 5b) presented breakage of intermolecular interactions and tearing into two structures. β-sheet intermolecular interactions were observed in all four simulated models. The forces that stabilize the fibril-like structures along the fibril axis include intermolecular hydrogen bonding between the β-arch peptides and aromatic interactions between the Phe groups. Along the fibril cross-section salt-bridge interactions between Glu and Lys stabilize the fibril-like structures (Figures S3, S4).

While in the simulated D-phosphopeptide fibril-like structures the β-hairpins demonstrate relatively rigid plated organization, the four models of the L-phosphopeptide revealed twisted structural features of the β-arch, similarly to as seen in the cross-β structural features in amyloids. Interestingly, both fibril-like structures in which the pSer are oriented in the outer domain of the fibril allowed for conservation of a tubular structure of similar diameter to that estimated by the TEM, whereas only one fibril-like structure in which the pSer is orientated in the inner domain of the fibril allowed for conservation of the tubular structure, also of similar diameter. MD simulation of all four models resulted in twisting and loosening of intermolecular interactions, which in some points along the fibril axis led to opening or partial opening of the tubular fibrils (Figure 5a–d). We propose that a combination of many opened or partially opened fibril-like structures as seen in the four models can lead to the supramolecular structures (Figure 5e) of nanotapes that resemble cinnamon sticks in shape, seen by microscopy.

Similarly to the D-phosphopeptide nanostructures, X-ray scattering was performed for the L-phosphopeptide nanostructures (Figure 5f). This spectrum, however, is different from that of D-phosphopeptide nanosheets and much more complex, with a multitude of prominent scattering peaks. The spectrum indicates crystallinity, though is difficult to resolve. In this case too, MD simulations were beneficial, and explained the complexity of the scattering spectrum. The two

suggested types of the L-phosphopeptide β-arch turns illustrated more flexibility compared to the turn in the D-phosphopeptide β-hairpin, and thus yielded polymorphic states from different organizations of the L-phosphopeptide. We therefore suggest that the multiple peaks in the X-ray scattering spectrum may be explained due to the polymorphic states and conformational change between various structures.

To confirm the significance of the phosphate group in the self-assembly process, the corresponding nonphosphorylated peptides were placed in the same self-assembly conditions as the phosphopeptides. The "D-peptide" (composed of L-amino acids and D-proline) formed a viscous liquid and fine fibers. The "L-peptide" gave rounded structures with undefined boundaries (Figure S5). In addition, no crystallinity or repeating distances were observed for the nonphosphorylated nanostructures by X-ray scattering analysis. The phosphate group was therefore demonstrated to be significant in the intermolecular interactions, molecular packing and self-assembly process, which is consistent with previously observed effects of phosphorylation.

CONCLUSIONS

We have described the self-assembly of nanostructures by two bioinspired amphiphilic phosphodecapeptides that differ only in the stereochemistry of a central proline residue. Secondary structure analysis indicated folded peptides with intramolecular β-sheets, and NMR gave indication of the presence of folded conformations in solution. The two phosphopeptides were placed in identical conditions for self-assembly, and while both peptides initiated their assembly process with formation of spherical structures, following a series of structural transitions, the nanostructures formed were markedly different, with nanosheets possessing a distinct half-elliptical shape formed by the D-phosphopeptide, and curved nanotapes formed by the L-phosphopeptide. It is noteworthy here that in organic solvent, prior to self-assembly into supramolecular structures, the predominant intra- and intermolecular forces would most likely be aromatic, van der Waals and electrostatic forces as well as hydrogen bonding. Because of the general amphiphilic nature of the peptides, together with presence of hydrophobic and aromatic phenylalanine residues, on addition of water hydrophobic interactions may compete with the aromatic and other intermolecular interactions as the predominant driving force for self-assembly. This could partially explain the gradual molecular reorganization and structural transitions. Our inspiration was nature's phospholipids and their self-assembly into various natural and synthetic molecular arrangements. The two-tailed phosphopeptides, with their additional peptidic features, present increased possibilities of intermolecular interactions, and therefore organize into additional molecular arrangements, which were significantly influenced by phosphorylation of a central serine residue.

MD simulation demonstrates an interesting possible mechanism of structural transition, whereby planar, untwisted β-hairpin molecules lie relatively flat. According to this simulation model, tubular structures undergo reshaping into polygonal structures. Flat polygons could provide insight into their possible interactions and organization to give the half-elliptical shapes observed. The high flexibility of the half-ellipses may also indicate their robustness, *i.e.,* there are instances where folding of the half-ellipses are observed by microscopy, which does not lead to their tearing.

The formation of complete nanotubes by the L-phosphopeptide in these conditions was not observed, and it is difficult to determine whether the nanostructures should be considered incomplete tubes or fully formed tapes. MD simulations of the L-phosphopeptide provided insight into a possible mechanism of formation of the curved tape structures. According to this simulation, during the transition process, the tubular fibril-like structures twist, and there is weakening of intermolecular interactions and opening or partial opening of the tubular fibril structures into open yet curved structures. New intermolecular interactions formed with additional opened structures could eventually lead to formation of the curved nanotapes we observed by microscopy.

In conclusion, the bioinspired design of phosphopeptides has led to new self-assembled nanostructures, and we have alluded to new possible mechanisms of self-assembly. Creation of new peptide assemblies continues to advance the field of synthetic biology, for development of novel biocompatible devices for a variety of biomedical applications.

METHODS

Preparation of Peptide Nanostructures. The phosphodecapeptides and nonphosphorylated analogues were purchased from Peptide 2.0. The lyophilized powder was dissolved in hexafluoroisopropanol (100 mg/mL, 5 μL). The concentrated peptide solutions were then diluted to a total concentration of 5 mg/mL with deionized water.

Secondary Structure Characterization. Circular dichroism was performed in TFE solution (0.05 mg/mL, 36.6 μM) in a 2 mm quartz cuvette, using a Chirascan circular dichroism spectrometer (Applied Photophysics Ltd.). Fourier transform infrared spectroscopy (FTIR) was performed for a sample peptide solution in TFE that was vacuum-dried on a polyethylene film, with trace quantities of water by deuterium exchange. A Nicolet Nexus 470 FTIR spectrometer with a deuterated triglycine sulfate detector was used, and measurements were taken using 4 cm^{-1} resolution and by averaging 32 scans. The obtained absorption spectra were smoothed by applying the Savitzky-Golay function.

Nanostructure Characterization. Transmission electron microscopy was performed using a Jeol JEM 1200EX electron microscope,

operating at 80 kV. Scanning electron microscopy was performed following gold coating, using a Jeol JSM 6300 scanning electron microscope. FTIR was performed for the aqueous nanostructure suspensions, similarly to the TFE solutions in characterizing secondary structure.

Construction of Self-Assembled Peptides and Molecular Dynamics (MD) Simulations. The details of construction of L- and D-phosphopeptides are described in the Supporting Information. The constructed self-assembled peptides had been simulated applying explicit MD simulations. The MD simulations protocol is described in detail in the Supporting Information.

X-ray Scattering Experiments (WAXS). Samples at 5 mg/mL concentration were centrifuged and measured in 1.5 mm diameter sealed quartz capillaries. Measurements were performed using an in-house X-ray scattering system, with a GeniX (Xenocs) low divergence Cu Kα radiation source (wavelength of 1.54 Å) and a scatterless slits setup.[51] Two-dimensional scattering data, with a momentum transfer wave vector (q) range of 0.8−22.0 nm^{-1} at a sample-to-detector distance of about 200 mm, was collected on a Pilatus 300 K detector (Dectris), and radially integrated using Matlab (MathWorks) based procedures (SAXSi). Experiments showed no radiation damage over 2 h of measurements. Background scattering data was collected from buffer solution alone.

Conflict of Interest: The authors declare no competing financial interest.

Acknowledgment. We are extremely grateful to R. Creasey at Nottingham University for her AFM imaging and measurements. The authors also thank J. Chill at Bar-Ilan University for his valuable discussions on interpretation of NMR spectra, and also A. Ginsberg at the Hebrew University of Jerusalem for his helpful discussion. We thank all the members of the Gazit laboratory for their helpful discussion and advice. Y.M. is funded by the FP7-PEOPLE-2011-CIG, research grant no. 303741. All simulations were performed using the high-performance computational facilities of the Miller lab in the BGU HPC computational center. The support of the BGU HPC computational center staff is greatly appreciated. R.B. acknowledges support by the Israeli Science Foundation (ISF 571/11), the European Community's seventh Framework Programme (CIG-293402) research grants and the Sackler Institute for Biophysics at Tel Aviv University.

Supporting Information Available: Tables S1−S5 (NMR Data); Figures S1−S5; computation details. This material is available free of charge *via* the Internet at http://pubs.acs.org.

REFERENCES AND NOTES

1. Klösgen, B. Conformations of Fluid Lipid Membranes. In *Lipid Bilayers*; Springer: Berlin, 2001; pp 47−88.
2. Schnur, J. M. Lipid Tubules: A Paradigm for Molecularly Engineered Structures. *Science* **1993**, *262*, 1669–1676.
3. Karlsson, A.; Karlsson, R.; Karlsson, M.; Cans, A.-S.; Stromberg, A.; Ryttsen, F.; Orwar, O. Molecular Engineering: Networks of Nanotubes and Containers. *Nature* **2001**, *409*, 150–152.
4. Adler-Abramovich, L.; Gazit, E. The Physical Properties of Supramolecular Peptide Assemblies: From Building Block Association to Technological Applications. *Chem. Soc. Rev.* **2014**, *43*, 6881–6893.
5. Mandal, D.; Nasrolahi Shirazi, A.; Parang, K. Self-Assembly of Peptides to Nanostructures. *Org. Biomol. Chem.* **2014**, *12*, 3544–3561.
6. Knowles, T. P.; Buehler, M. J. Nanomechanics of Functional and Pathological Amyloid Materials. *Nat. Nanotechnol.* **2011**, *6*, 469–479.
7. Verkleij, A. J. Lipidic Intramembranous Particles. *Biochim. Biophys. Acta, Rev. Biomembr.* **1984**, *779*, 43–63.
8. Loomis, K.; McNeeley, K.; Bellamkonda, R. V. Nanoparticles with Targeting, Triggered Release, and Imaging Functionality for Cancer Applications. *Soft Matter* **2011**, *7*, 839–856.
9. Lim, S. B.; Banerjee, A.; Önyüksel, H. Improvement of Drug Safety by the Use of Lipid-Based Nanocarriers. *J. Controlled Release* **2012**, *163*, 34–45.
10. Valetti, S.; Mura, S.; Stella, B.; Couvreur, P. Rational Design for Multifunctional Non-Liposomal Lipid-Based Nanocarriers for Cancer Management: Theory to Practice. *J. Nanobiotechnol.* **2013**, *11*, S6.
11. Shimizu, T.; Masuda, M.; Minamikawa, H. Supramolecular Nanotube Architectures Based on Amphiphilic Molecules. *Chem. Rev.* **2005**, *105*, 1401–1444.
12. Shimizu, T. Molecular Self-Assembly into One-Dimensional Nanotube Architectures and Exploitation of Their Functions. *Bull. Chem. Soc. Jpn.* **2008**, *81*, 1554–1566.
13. Zhang, S. Lipid-Like Self-Assembling Peptides. *Acc. Chem. Res.* **2012**, *45*, 2142–2150.
14. Cavalli, S.; Albericio, F.; Kros, A. Amphiphilic Peptides and Their Cross-Disciplinary Role as Building Blocks for Nanoscience. *Chem. Soc. Rev.* **2010**, *39*, 241–263.
15. Hamley, I. W. Self-Assembly of Amphiphilic Peptides. *Soft Matter* **2011**, *7*, 4122–4138.
16. Xu, H.; Wang, J.; Han, S.; Wang, J.; Yu, D.; Zhang, H.; Xia, D.; Zhao, X.; Waigh, T. A.; Lu, J. R. Hydrophobic-Region-Induced Transitions in Self-Assembled Peptide Nanostructures. *Langmuir* **2008**, *25*, 4115–4123.
17. Meng, Q.; Kou, Y.; Ma, X.; Liang, Y.; Guo, L.; Ni, C.; Liu, K. Tunable Self-Assembled Peptide Amphiphile Nanostructures. *Langmuir* **2012**, *28*, 5017–5022.
18. Cui, H.; Webber, M. J.; Stupp, S. I. Self-Assembly of Peptide Amphiphiles: From Molecules to Nanostructures to Biomaterials. *Biopolymers* **2010**, *94*, 1–18.
19. Hule, R. A.; Nagarkar, R. P.; Altunbas, A.; Ramay, H. R.; Branco, M. C.; Schneider, J. P.; Pochan, D. J. Correlations between Structure, Material Properties and Bioproperties in Self-Assembled β-Hairpin Peptide Hydrogels. *Faraday Discuss.* **2008**, *139*, 251–264.
20. Rajagopal, K.; Lamm, M. S.; Haines-Butterick, L. A.; Pochan, D. J.; Schneider, J. P. Tuning the pH Responsiveness of β-Hairpin Peptide Folding, Self-Assembly, and Hydrogel Material Formation. *Biomacromolecules* **2009**, *10*, 2619–2625.
21. Reches, M.; Gazit, E. Casting Metal Nanowires within Discrete Self-Assembled Peptide Nanotubes. *Science* **2003**, *300*, 625–627.
22. Yan, X.; Zhu, P.; Li, J. Self-Assembly and Application of Diphenylalanine-Based Nanostructures. *Chem. Soc. Rev.* **2010**, *39*, 1877–1890.
23. Song, X.; Geiger, C.; Farahat, M.; Perlstein, J.; Whitten, D. G. Aggregation of Stilbene Derivatized Fatty Acids and Phospholipids in Monolayers and Vesicles. *J. Am. Chem. Soc.* **1997**, *119*, 12481–12491.
24. Whitten, D. G.; Chen, L.; Geiger, H. C.; Perlstein, J.; Song, X. Self-Assembly of Aromatic-Functionalized Amphiphiles: The Role and Consequences of Aromatic-Aromatic Noncovalent Interactions in Building Supramolecular Aggregates and Novel Assemblies. *J. Phys. Chem. B* **1998**, *102*, 10098–10111.
25. Marsh, D. Thermodynamics of Phospholipid Self-Assembly. *Biophys. J.* **2012**, *102*, 1079–1087.
26. Grundke-Iqbal, I.; Iqbal, K.; Tung, Y. C.; Quinlan, M.; Wisniewski, H. M.; Binder, L. I. Abnormal Phosphorylation of the Microtubule-Associated Protein t (Tau) in Alzheimer Cytoskeletal Pathology. *Proc. Natl. Acad. Sci. U. S. A.* **1986**, *83*, 4913–4917.
27. Lee, M.-S.; Kao, S.-C.; Lemere, C. A.; Xia, W.; Tseng, H.-C.; Zhou, Y.; Neve, R.; Ahlijanian, M. K.; Tsai, L.-H. APP Processing Is Regulated by Cytoplasmic Phosphorylation. *J. Cell Biol.* **2003**, *163*, 83–95.
28. Inoue, M.; Konno, T.; Tainaka, K.; Nakata, E.; Yoshida, H.-o.; Morii, T. Positional Effects of Phosphorylation on the Stability and Morphology of Tau-Related Amyloid Fibrils. *Biochemistry* **2012**, *51*, 1396–1406.
29. Signarvic, R. S.; DeGrado, W. F. *De Novo* Design of a Molecular Switch: Phosphorylation-Dependent Association of Designed Peptides. *J. Mol. Biol.* **2003**, *334*, 1–12.
30. Broncel, M.; Wagner, S. C.; Hackenberger, C. P. R.; Koksch, B. Enzymatically Triggered Amyloid Formation: An Approach for Studying Peptide Aggregation. *Chem. Commun.* **2010**, *46*, 3080–3082.

31. Yang, Z.; Liang, G.; Wang, L.; Xu, B. Using a Kinase/Phosphatase Switch to Regulate a Supramolecular Hydrogel and Forming the Supramolecular Hydrogel *in Vivo*. *J. Am. Chem. Soc.* **2006**, *128*, 3038–3043.
32. Webber, M. J.; Newcomb, C. J.; Bitton, R.; Stupp, S. I. Switching of Self-Assembly in a Peptide Nanostructure with a Specific Enzyme. *Soft Matter* **2011**, *7*, 9665–9672.
33. Kühnle, H.; Börner, H. G. Biotransformation on Polymer–Peptide Conjugates: A Versatile Tool to Trigger Microstructure Formation. *Angew. Chem., Int. Ed.* **2009**, *48*, 6431–6434.
34. Tatko, C. D.; Waters, M. L. Selective Aromatic Interactions in β-Hairpin Peptides. *J. Am. Chem. Soc.* **2002**, *124*, 9372–9373.
35. Roy, R. S.; Gopi, H. N.; Raghothama, S.; Gilardi, R. D.; Karle, I. L.; Balaram, P. Peptide Hairpins with Strand Segments Containing α- and β-Amino Acid Residues: Cross-Strand Aromatic Interactions of Facing Phe Residues. *Biopolymers* **2005**, *80*, 787–799.
36. Rajagopal, A.; Aravinda, S.; Raghothama, S.; Shamala, N.; Balaram, P. Aromatic Interactions in Model Peptide β-Hairpins: Ring Current Effects on Proton Chemical Shifts. *Biopolymers* **2012**, *98*, 185–194.
37. Makwana, K. M.; Mahalakshmi, R. Comparative Analysis of Cross Strand Aromatic-Phe Interactions in Designed Peptide β-Hairpins. *Org. Biomol. Chem.* **2014**, *12*, 2053–2061.
38. Mahalakshmi, R.; Raghothama, S.; Balaram, P. NMR Analysis of Aromatic Interactions in Designed Peptide β-Hairpins. *J. Am. Chem. Soc.* **2006**, *128*, 1125–1138.
39. Waters, M. L. Aromatic Interactions in Peptides: Impact on Structure and Function. *Biopolymers* **2004**, *76*, 435–445.
40. Sonnichsen, F. D.; Van Eyk, J. E.; Hodges, R. S.; Sykes, B. D. Effect of Trifluoroethanol on Protein Secondary Structure: An NMR and CD Study Using a Synthetic Actin Peptide. *Biochemistry* **1992**, *31*, 8790–8798.
41. Zhong, L.; Johnson, W. C. Environment Affects Amino Acid Preference for Secondary Structure. *Proc. Natl. Acad. Sci. U. S. A.* **1992**, *89*, 4462–4465.
42. Xiao, J.; Weisblum, B.; Wipf, P. Trisubstituted (E)-Alkene Dipeptide Isosteres as β-Turn Promoters in the Gramicidin S Cyclodecapeptide Scaffold. *Org. Lett.* **2006**, *8*, 4731–4734.
43. Gibbs, A. C.; Kondejewski, L. H.; Gronwald, W.; Nip, A. M.; Hodges, R. S.; Sykes, B. D.; Wishart, D. S. Unusual β-Sheet Periodicity in Small Cyclic Peptides. *Nat. Struct. Mol. Biol.* **1998**, *5*, 284–288.
44. Hennetin, J.; Jullian, B.; Steven, A. C.; Kajava, A. V. Standard Conformations of β-Arches in β-Solenoid Proteins. *J. Mol. Biol.* **2006**, *358*, 1094–1105.
45. Reches, M.; Gazit, E. Designed Aromatic Homo-Dipeptides: Formation of Ordered Nanostructures and Potential Nanotechnological Applications. *Phys. Biol.* **2006**, *3*, S10.
46. Segman-Magidovich, S.; Lee, M.-r.; Vaiser, V.; Struth, B.; Gellman, S. H.; Rapaport, H. Sheet-Like Assemblies of Charged Amphiphilic α/β-Peptides at the Air–Water Interface. *Chem.—Eur. J.* **2011**, *17*, 14857–14866.
47. Powers, E. T.; Yang, S. I.; Lieber, C. M.; Kelly, J. W. Ordered Langmuir–Blodgett Films of Amphiphilic β-Hairpin Peptides Imaged by Atomic Force Microscopy. *Angew. Chem., Int. Ed.* **2002**, *41*, 127–130.
48. Hamley, I. W.; Dehsorkhi, A.; Castelletto, V. Self-Assembled Arginine-Coated Peptide Nanosheets in Water. *Chem. Commun.* **2013**, *49*, 1850–1852.
49. Vauthey, S.; Santoso, S.; Gong, H.; Watson, N.; Zhang, S. Molecular Self-Assembly of Surfactant-Like Peptides to Form Nanotubes and Nanovesicles. *Proc. Natl. Acad. Sci. U. S. A.* **2002**, *99*, 5355–5360.
50. Cenker, C. C.; Bomans, P. H. H.; Friedrich, H.; Dedeoglu, B.; Aviyente, V.; Olsson, U.; Sommerdijk, N. A. J. M.; Bucak, S. Peptide Nanotube Formation: A Crystal Growth Process. *Soft Matter* **2012**, *8*, 7463–7470.
51. Li, Y.; Beck, R.; Huang, T.; Choi, M. C.; Divinagracia, M. Scatterless Hybrid Metal-Single-Crystal Slit for Small-Angle X-Ray Scattering and High-Resolution X-Ray Diffraction J. Appl. Crystallogr. **2008**, *41*, 1134–1139.